Environmental Science
Processes & Impacts

Accepted Manuscript

ROYAL SOCIETY OF CHEMISTRY

rsc.li/process-impacts

Table of Contents

Direct *in Situ* Measurement of Dissolved Zinc in the Presence of Zinc Oxide Nanoparticles Using Anodic Stripping Voltammetry

*Chuanjia Jiang, Heileen Hsu-Kim**

Department of Civil and Environmental Engineering, Box 90287, Duke University, NC 27708

*Corresponding author: Heileen Hsu-Kim. Email: hsukim@duke.edu. Phone +1-919-660-5109

Anodic stripping voltammetry can measure dissolved zinc concentration in aqueous suspensions of ZnO nanoparticles with primary particle diameters of 20 nm or larger.

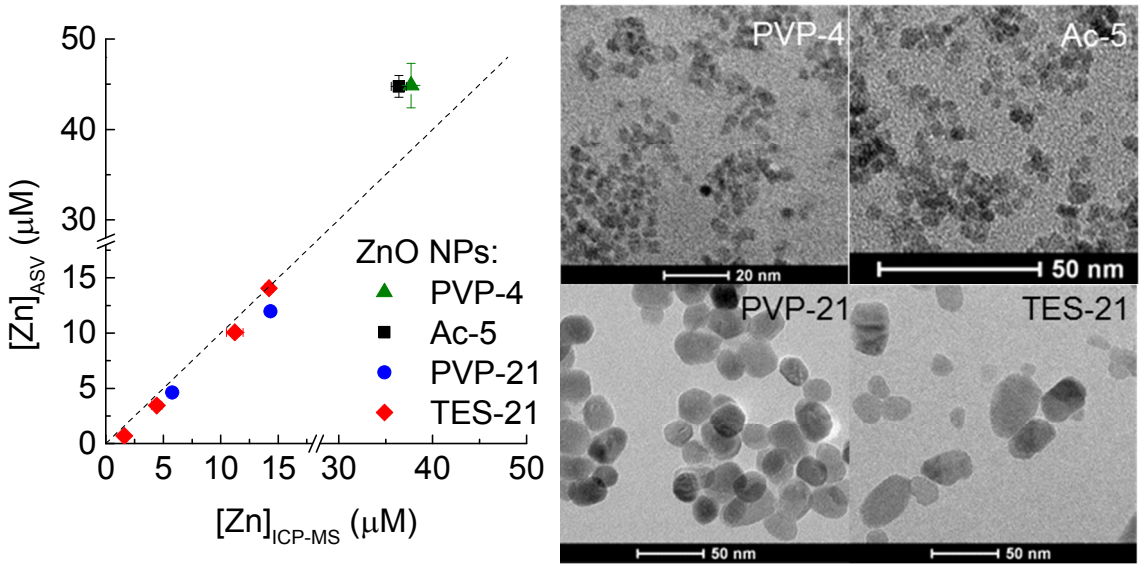

Environmental Impact Statement

With the rapid development of nanotechnology, increasingly larger amounts of engineered nanomaterials such as zinc oxide (ZnO) nanoparticles (NPs) are released into the environment and have become an important class of emerging contaminants. The fate and toxicity of metal-based nanomaterials including ZnO NPs in aquatic environments often depend on the dissolution process, the rate of which is influenced by many environmental factors and thus difficult to quantify in complex environmental media. This paper demonstrates that anodic stripping voltammetry can be used to measure dissolved zinc concentration in the presence of ZnO NPs and serve as a useful tool to study the dissolution kinetics of metal-based NPs.

Direct *in Situ* Measurement of Dissolved Zinc in the Presence of Zinc Oxide Nanoparticles Using Anodic Stripping Voltammetry

*Chuanjia Jiang, Heileen Hsu-Kim**

Department of Civil and Environmental Engineering, Box 90287, Duke University, NC 27708

*Corresponding author: Heileen Hsu-Kim. Email: hsukim@duke.edu. Phone +1-919-660-5109

Abstract: The wide use of metal-based nanomaterials such as zinc oxide (ZnO) nanoparticles (NPs) has generated concerns regarding their environmental and health risks. For ZnO NPs, their toxicity in aquatic systems often depends on the release of dissolved zinc species, and the rate of dissolution is influenced by water chemistry, including the presence of zinc-chelating ligands. A challenge, however, remains in quantifying the dissolution of ZnO NPs, particularly for time scales that are short enough to determine rates. This paper reports the application of anodic stripping voltammetry (ASV) with a hanging mercury drop electrode to directly measure the concentration of dissolved zinc in ZnO NP suspensions, without separation of the ZnO NPs from the aqueous phase. The effects of deposition time and the electrochemical potential scan rate on the ASV measurement were consistent with expectations for dissolved phase measurements. Dissolved zinc concentration measured by ASV ($[Zn]_{ASV}$) was compared with that measured by inductively coupled plasma mass spectrometry (ICP-MS) after ultracentrifugation ($[Zn]_{ICP-MS}$), for four types of ZnO NPs with different coatings and primary particle diameters. For small ZnO NPs (4-5 nm), $[Zn]_{ASV}$ was 20% higher than $[Zn]_{ICP-MS}$, suggesting that these small NPs contributed to the voltammetric measurement. For larger ZnO NPs (approximately 20 nm), $[Zn]_{ASV}$ was (79±19)% of $[Zn]_{ICP-MS}$, despite the high concentrations of ZnO NPs in suspension. Using ASV, the dissolution of ZnO NPs was studied, with or without Suwannee River fulvic acid (SRFA). Although SRFA diminished the ASV stripping current, dissolution of 20 nm ZnO NPs was significantly promoted at high fulvic acid to ZnO NP ratios. The ASV method described in this paper provides a useful tool for studying the dissolution kinetics of ZnO NPs in complex environmental matrices.

Introduction

Engineered nanomaterials (ENMs) of different chemical compositions (e.g. carbonaceous, metal and metal oxide, etc.) have become a class of emerging pollutants with known or potential environmental, health, and safety implications.[1] Among these ENMs, zinc oxide (ZnO) nanoparticles (NPs) are widely used in many consumer and industrial products, such as sunscreen, pigment, food additives, photocatalyst for pollution control, and antimicrobial agents.[2-4] However, ZnO NPs have been found to be toxic to various taxa of aquatic and terrestrial living organisms.[5]

The toxicity of ZnO NPs can often be attributed to the release of dissolved zinc ions from the nanoparticles,[6-13] while some other studies found that dissolution alone cannot explain the observed toxicity, with undissolved ZnO NPs also likely to play a role.[14-17] Thus, dissolution of ZnO NPs is very important in studying its toxicity, and has been examined in many of the toxicological studies. The determination of dissolved zinc concentration in a suspension of nanoparticles first requires separation of the dissolved phase from the particles prior to analysis by atomic spectrometry (e.g., atomic absorption spectrometry, inductively coupled plasma atomic emission spectroscopy), or inductively coupled plasma mass spectrometry (ICP-MS). Examples of separation procedures include equilibrium dialysis,[6] membrane filtration (with nominal size cut-offs),[7, 14] ultracentrifugation,[8, 16] centrifugal ultrafiltration [11, 17] or a combination of ultracentrifugation and filtration.[9, 12] Interpretation of these methods can be challenging, however, as the separation of dissolved molecules from the original nanoparticles may be incomplete, resulting in measurement inaccuracy.[18, 19] Furthermore, these separation methods can be relatively time consuming, which makes them less suitable for kinetic studies of dissolution, especially with ZnO NPs.[18]

To address these limitations, voltammetric techniques have been used to study the solubility and dissolution kinetics of ZnO NPs. For example, a technique called Absence of Gradients and Nernstian Equilibrium Stripping (AGNES)[18] was developed to measure the concentration of free zinc ion (Zn^{2+}) *in situ* at a high time resolution. From this measurement, the concentration of total dissolved zinc species must then be inferred from equilibrium calculations using the measured Zn^{2+} concentration and stability constants of zinc-complexing ligands in the solution. While this approach may be suitable for solutions with well-defined metal speciation, the AGNES technique cannot be used to measure the solubility of ZnO NP in the presence of ligands with unknown or poorly defined stability constants. An example is natural organic matter (NOM), which plays a key role in the dissolution and transformation of metal-bearing NPs and colloids in environmental systems.[20]

Here we report the application of anodic stripping voltammetry (ASV) with a hanging mercury drop electrode (HMDE) to directly measure the concentration of dissolved zinc in a suspension of ZnO NPs, both in the absence and presence of NOM. ASV has been successfully used in numerous studies to measure dissolved zinc concentration with high sensitivity and precision[21-23] even in matrices with high content of organic matter.[24] However, the interpretation of voltammetry data for samples containing very small particles can be uncertain. For example, some researchers have shown that zinc and other metals bound to inorganic colloidal/particulate phase (including zinc sulfide NPs[25]) are undetectable by ASV and other voltammetric techniques (e.g. adsorptive cathodic stripping voltammetry and cyclic voltammetry),[21, 26-30] while other studies have indicated that metal-containing nanoparticles may produce a signal during voltammetric scans.[31-33] The voltammetric signal of nanoparticles would depend not only on concentration, but also on particle size, crystallinity, and aggregation state and therefore cannot

be calibrated with concentration in environmental matrices. The feasibility of ASV to quantify dissolved zinc concentration *in situ*, i.e. in the presence of ZnO NPs, has yet to be reported and is the objective of this study. ASV was used to measure the dissolution of several types of ZnO NPs with a range of primary particle diameter (all less than 30 nm) and surface coatings. ASV measurements were compared to ultracentrifugation followed by ICP-MS. Tests were also performed to discern the effects of dissolved NOM and pH for nanoparticle dissolution measurements.

Experimental

Materials.

All chemicals used in the study were ACS grade and purchased from Sigma-Aldrich, unless stated otherwise. Trace metal grade concentrated nitric acid (HNO_3) and hydrochloric acid (HCl) were purchased from Fisher Scientific. Suwannee River fulvic acid (SRFA) standard (Catalog No.: 2S101F) was purchased from the International Humic Substances Society. A stock solution was made by dissolving SRFA powder in ultrapure water (> 17.8 MΩ·cm, Barnstead Nanopure, Thermo Scientific, US), adjusting the pH to 6-7 with sodium hydroxide (NaOH, Mallinckrodt Baker), and filtering through 0.2 μm Nylon membrane syringe filter (VWR International). The concentration of SRFA in the stock solution was determined as Non-purgeable Organic Carbon (NPOC) using a Total Organic Carbon (TOC) Analyzer (TOC-L CPN, Shimadzu, Japan).

Four ZnO NP stocks of different primary particle sizes were used in this study, including 3 laboratory-synthesized ZnO NPs coated with acetate or polyvinylpyrrolidone (PVP) and a commercial ZnO NP (catalog No. 721077, Sigma-Aldrich) which was coated with cationic 3-

aminopropyl triethoxysilane (APTES). In this study, we referred to these ZnO NPs using their coatings and average primary particle size in nanometers: PVP-4, Ac-5, PVP-21 and TES-21 (**Table 1**). TES-21 ZnO NP was received as a concentrated aqueous dispersion and was diluted to working stock dispersions of about 20 mM (pH = 7.6-7.7), the exact concentration of which was measured by ICP-MS (Agilent 7700x, Agilent Technologies) after digestion in mixed acid (2% HNO_3 and 0.5% HCl) overnight at room temperature. The other 3 ZnO NPs were dispersed in ethanol or ultrapure water, and their synthesis procedures are summarized in the following section and described in detail in Supporting Information. The ZnO NP stock suspensions were stored at 4 °C; before their use in experiments, the stocks were sonicated and returned to room temperature. Dissolved zinc concentration in the ZnO NP stock suspensions was measured by ICP-MS after ultracentrifugation (method and results are given in the Supporting Information).

A surface water sample was obtained from the constructed freshwater wetland mesocosms located in Duke Forest (36º1'30"N, 78º59'4"W), Durham, North Carolina and used as a matrix for a dissolved Zn experiment. This simulated wetland was constructed according to a previously described study [34] and designed to investigate the long term environmental aquatic fate and toxicity of engineered nanomaterials. Surface water from the mesocosm was collected in July 2014, prior to dosing with nanomaterials. The surface water was serially filtered through 0.45 and 0.1 μm membrane filters (HAWP02500 and VCWP02500, Millipore) and purged with nitrogen prior to use as a matrix for ZnO NP dissolution measurements.

Before filtration, the pH of the wetland water was 6.8; after filtration, the pH was 7.1. TOC concentration in the filtered wetland water was 16.7±0.6 mg-C L^{-1}. Metal/metalloid concentrations in the filtered wetland water were measured by ICP-MS (**Table S2** and **Table S3**, for elements > 0.1 μM and <0.1 μM, respectively), and zinc concentration in the water was < 0.1

μM (**Table S3**). Based on the measured metal concentrations (**Table S2**), the ionic strength of the filtered wetland water was estimated to be approximately 1 mM.

Synthesis and characterization of ZnO NPs. As described in detail in the Supporting Information, the acetate-coated ZnO NPs (Ac-5) were synthesized by hydrolysis of zinc acetate dihydrate with NaOH.[35] ZnO NPs synthesized using this method are likely to have acetate adsorbed on the surface, even after washing with hexane or heptane. This method was modified by the addition of PVP (55,000 average molecular weight) to the reaction mixture to produce PVP-coated ZnO NPs,[36] The primary particle size of the ZnO NPs was controlled by adding different amounts of water to the reaction mixture.[37]

The ZnO NPs were characterized by transmission electron microscopy (TEM) (FEI Tecnai) after the samples were deposited on a copper grid with carbon film. The average primary particle diameter (d_{TEM}) was determined by measuring the size of about 180 to 730 NPs in TEM images for each type of ZnO NP. The ZnO NPs were also deposited and dried on amorphous glass slides and characterized by X-ray diffraction (XRD) (Panalytical X'pert PRO MRD) to determine the crystal structure. Crystallite size (d_c) of the ZnO NPs was estimated from the diffraction peak broadening at $2\theta = 56.6^{o}$ (corresponding to the (110) crystal planes), according to the Debye-Scherrer equation.

$$d_c = (k\,\lambda)/(\beta\,\cos\theta)$$

where k is a constant (k=0.89); λ is the wavelength of Cu Kα X-ray (λ=0.154 nm); β is the full width at half-maximum (FWHM) of the diffraction peaks (in radians); θ is the Bragg diffraction angle.

Dynamic Light Scattering (DLS) was used to measure the average hydrodynamic diameter (d_h) of ZnO NPs in stock suspensions as well as the aggregation kinetics in KCl

solution. DLS was performed using a Zetasizer Nano-ZS instrument (ZEN3600, Malvern Instruments), and Z-average hydrodynamic diameter was measured by analyzing the intensity fluctuations of light (wavelength = 663 nm) backscattered at 173°.

ASV instrument setup. The voltammetric system consisted of a Metrohm 663 VA Stand (Metrohm) controlled by the μAutolab Type III potentiostat (Eco Chemie, Netherlands) with the IME663 interface and the General Purpose Electrochemical System (GPES) software (version 4.9). The working electrode was a Metrohm Multi Mode Electrode Pro (MME Pro) operated in Static Mercury Drop Electrode mode. A saturated calomel electrode was used as the reference electrode, and a platinum wire used as counter electrode. Dissolution experiments and ASV measurements took place in a temperature-controlled glass electrochemical cell, which was covered with aluminum foil to avoid direct light illumination. Temperature was controlled at 25.0±0.1 ºC by a recirculating water bath (Isotemp, Fisher Scientific).

ASV measurement and dissolution experiment. Dissolution experiments of the 4 ZnO NPs were performed in KCl solutions (81-91 mM) buffered with 3-(*N*-morpholino)-propanesulfonic acid (MOPS) (20 mM) or Piperazine-*N*,*N*'-bis(2-hydroxypropanesulfonic acid (POPSO) (5 and 10 mM), at ionic strength I = 0.1 M, pH = 7.9-8.6 and 25.0±0.1 ºC, with or without SRFA. In one experiment, an aliquot of the filtered wetland water was used as the sample matrix.

In each dissolution experiment, 50 mL of the buffered KCl solution or wetland surface water was dispensed into the electrochemical cell and deaerated by purging with water-saturated ultra-high-purity N_2 for more than 5 min. Then, an ASV measurement was taken as a Zn blank and to ensure no traces of O_2. After the blanks were taken, a certain volume (typically < 0.2 mL)

of ZnO NP stock was added to the electrochemical cell, and the time was recorded with a precision of 1 to 2 s. Then ASV measurements were taken at different time points.

Each ASV measurement was performed with a freshly produced hanging mercury drop and consisted of three steps. In the first step (the deposition step), the electrode potential was held at -1.4 V under stirring for a controlled period of deposition time (10 s in this study), and a small portion of dissolved zinc ions in solution was reduced to elemental zinc, forming an amalgam on the surface of the mercury electrode. In this step, zinc was preconcentrated onto the electrode, ensuring high sensitivity, and the preconcentration factor depended on the deposition time. Then in the second step, 5 s was allowed for equilibrium or conditioning, and the electrode potential was held at -1.4 V without stirring during this time. In the last step (the stripping step), the electrode potential was scanned linearly from -1.4 V to 0 V at a scan rate of 0.1 V s^{-1}, and the elemental zinc in the amalgam was reoxidized and stripped out of the electrode at about -1.0 V, resulting in a peak on the voltammogram. Between each time point, the solution was stirred and purged with water-saturated N_2 to enhance mass transfer. At the end of each dissolution experiment, the pH of the reaction mixture was measured, using a pH meter (Φ350, Beckman) with an automatic temperature compensation probe (Beckman Coulter). For some samples, an aliquot of the sample was removed and dispensed into mixed acid (2%HNO_3 and 0.5% HCl) for analysis of Zn by ICP-MS.

External calibration was performed on a daily basis for quantification of dissolved zinc ions, in the same matrix as the dissolution experiments. A Zn working stock solution (1.00 or 2.00 mM) used for calibration was made by diluting a 1000±5 mg-Zn L^{-1} zinc standard solution (in 3% HNO_3) (Ricca Chemicals) with ultrapure water. In making calibrations, Zn working stock

solution was added to the buffered matrix with increments of 20 to 50 μL, and one to three ASV measurements were taken after each addition to record the peak current (i.e., peak height) and peak area. For dissolution experiments with ZnO NPs dispersed in ethanol, the dissolved Zn calibrations were performed in the buffered KCl solution with the same volume of ethanol corresponding to the NP samples. Separate calibrations were also performed for matrices with added SRFA at different concentrations.

The limits of detection (LOD) of the ASV method with or without 20 mg-C L^{-1} SRFA were determined as 3 times the standard deviation of multiple measurements (N = 10) of a blank sample in corresponding buffered KCl solutions (I = 0.1 M, pH = 8.5-8.6, with or without 20 mg-C L^{-1} SRFA). With the above ASV parameters used (i.e. 10 s deposition time and 0.1 V s^{-1} scan rate), the LOD was 2×10^{-8} M with no NOM and 6×10^{-8} M with 20 mg-C L^{-1} SRFA, both of which are higher than the LOD values (e.g. 10^{-10} to 10^{-9} M)[22, 38] typical of ASV measurements with longer deposition times but low enough as compared to dissolved zinc concentration in the dissolution experiments.

Effects of deposition time and scan rate on ASV measurement. The above dissolution experiments were performed with fixed voltammetric parameters. A deposition potential of -1.4 V was chosen so that it was 0.3 to 0.4 V more negative than the reduction potential of zinc.[21, 39] Two other parameters, i.e. deposition time and potential scan rate, were tested for their effects on ASV measurement, in the presence of TES-21 ZnO NP in the KCl buffer solution. A longer deposition time enables higher sensitivity and lower LOD;[24] however, short deposition time allows for higher time resolution, which is a prerequisite for kinetic studies for ZnO NPs. For these tests, a diluted suspension of TES-21 ZnO NPs (total concentration of 85 μM) in the KCl buffer was prepared and allowed 2 h to reach equilibrium. Then ASV measurements were

performed under varying deposition times (between 2 and 100 s), with scan rate fixed at 0.1 V s^{-1} and also with varying scan rates (between 0.01 and 0.4 V s^{-1}) at a fixed 10 s deposition time. Dissolved zinc concentration in this reaction mixture was measured by the ASV peak current at -1.0 V. After these measurements, an aliquot of the sample was diluted in a mixed acid (2% HNO_3 and 0.5% HCl), held overnight at room temperature, and analyzed for total zinc concentration by ICP-MS.

Ultracentrifugation and ICP-MS analysis. Equilibrium dissolved zinc concentration measured by ASV was compared with that measured by ICP-MS after ultracentrifugation. ZnO NP suspensions of 75 to 290 μM were prepared by adding different volumes of ZnO NP stock suspensions to buffered KCl solution (I = 0.1 M, pH = 8.3-8.6), with or without SRFA, and allowed between 25 min (for PVP-4 and Ac-5 ZnO NPs) and up to 1.5 h (for TES-21 ZnO NPs) to reach equilibrium solubility at 25 ºC.

An additional sample of TES-21 ZnO NP (75 μM total zinc concentration) was prepared in filtered and N_2-purged wetland surface water. We note that the N_2 purging step did not change the pH of the KCl buffer solutions; however, purging did change the pH of the surface water sample (likely due to loss of CO_2, the major buffer for the natural water sample). Thus, the surface water sample was purged with N_2 for at least 3 h to maintain a stable pH value (pH 9) prior to amending with ZnO NPs. This sample was allowed to equilibrate in a N_2 atmosphere for 50 min at 25 ºC prior to analysis.

Dissolved zinc concentration in each of these ZnO NP samples was measured by ASV, and then two 4-mL aliquots of the ZnO NP suspensions were transferred to Ultra-Clear centrifuge tubes (Beckman Coulter, US) and centrifuged in duplicate at 60000 rpm (370000 g) and 25 ºC for 1 h (L8-80M, Beckman). The supernatant was digested in a 2% HNO_3 + 0.5% HCl

mixture, and zinc concentration was quantified by ICP-MS, with external calibration made using a multi-element trace metal standard (BDH Aristar plus, VWR International). Dissolved Zn calibration solutions and the ZnO NP stock suspensions were also subjected to ultracentrifugation and then analyzed for Zn in the supernatant by ICP-MS.

Results and Discussion

Characteristics of the ZnO NPs. The four ZnO NPs used in the study all comprised of roughly spheroidal particles (**Figure S1**). The three ZnO NPs made in our lab (i.e., PVP-4, Ac-5 and PVP-21) were more regular in shape and relatively monodisperse in primary particle size, while the commercial ZnO NPs (i.e. TES-21) were less regular in shape and had wider particle size distribution, as reflected by the larger standard deviation in primary particle diameter (d_{TEM}) along both the long and short axes (**Table 1**). All four ZnO NPs had wurtzite-like crystal structure, as determined from their XRD spectra (**Figure S2**), and crystallite size (d_c) was slightly smaller than d_{TEM} (**Table 1**).

The ZnO NPs were well dispersed in stock suspensions, without severe aggregation, and the Z-average hydrodynamic diameter (d_h) was generally 3-5 times larger than the average d_{TEM} value (**Table 1**). The stability of ZnO NP stock suspensions depended on the dispersion media, surface coating and ZnO NP concentration. The PVP-4 ZnO NP stock suspension, which was dispersed in ethanol, was stable over months (d_h = 20 nm after 186 d), while working stock suspensions of the two ZnO NPs dispersed in water (i.e. PVP-21 and TES-21) were stable for only a few weeks. For the Ac-5 ZnO NPs, the stability was strongly influenced by ZnO NP concentration. For a batch of Ac-5 ZnO NPs redispersed in 20 mL of ethanol (with a total concentration of 27 mM, as measured by ICP-MS after acid digestion), the stock suspension was

stable for months (d_h = 22 nm after 126 d), while for another batch redispersed in 12 mL of ethanol (with a total concentration of 75 mM), irreversible aggregation occurred within 77 d, with d_h = 98 nm, even after sonication. Aggregation rate depends on the particle number concentration; at higher concentrations, the collision probability is higher, thus leading to higher aggregation rates.[40] Moreover, concentrations of residual Na^+ and acetate ions were higher in the batch redispersed in 12 mL of ethanol, which may have contributed to the lower stability of the ZnO NP stock suspension.

Table 1. Summary of major characteristics of the ZnO NPs.

ZnO NP	Coating	Dispersion medium	d_{TEM} (nm)[a]	d_c (nm)[b]	d_h (nm)[c]
PVP-4	PVP	ethanol	4.2±0.7	4	16
Ac-5	acetate	ethanol	4.6±0.9	4	20 or 98[d]
PVP-21	PVP	water	20.7±4.7 (26.3±6.8) [e]	14	98
TES-21	APTES	water	21.3±8.0 (28.4±11.2) [e]	16	73

Notes:
[a] Primary particle diameter measured by TEM, given as arithmetic mean ± standard deviation.
[b] Crystallite size of the ZnO NPs estimated from XRD peak broadening according to the Debye-Scherrer equation.
[c] Z-average hydrodynamic diameter in working stock suspensions measured by DLS at the time of dissolution experiments.
[d] Two batches of Ac-5 ZnO NPs dispersed in different volumes of ethanol were used for dissolution experiments. For the batch redispersed in 20 mL of ethanol, d_h was 20 nm after sonication, while the batch redispersed in 12 mL of ethanol was highly aggregated, with d_h = 98 nm even after sonication.
[e] For these samples, numbers inside and outside the parentheses are average diameter measured along the long and short axes of the ZnO NPs, respectively.

Effects of deposition time and scan rate on ASV measurement. In a suspension of TES-21 ZnO NP with 4 μM dissolved zinc (85 μM total concentration), the stripping current during the ASV measurement increased with deposition time (**Figure 1**). The peak position shifted slightly from -1.04 V to -1.02 V as deposition time increased from 2 s to 100 s. When peak current was plotted versus deposition time plus the 5 s equilibrium time (**Figure 1b**), the

258 regression line from the first three data points (i.e. 2 s, 5 s and 10 s deposition time) crossed the
259 ordinate at 3.3×10^{-9} A, which was very close to the origin. For deposition times longer than 10 s,
260 the relationship between peak current and deposition time appeared to be non-linear. This trend
261 has been observed in the measurement of zinc and other metal ions using cathodic stripping
262 voltammetry with a HMDE, and has been explained by the approach to saturation of the mercury
263 drop surface at high metal concentrations (and high peak current signals).[41-46]
264
265

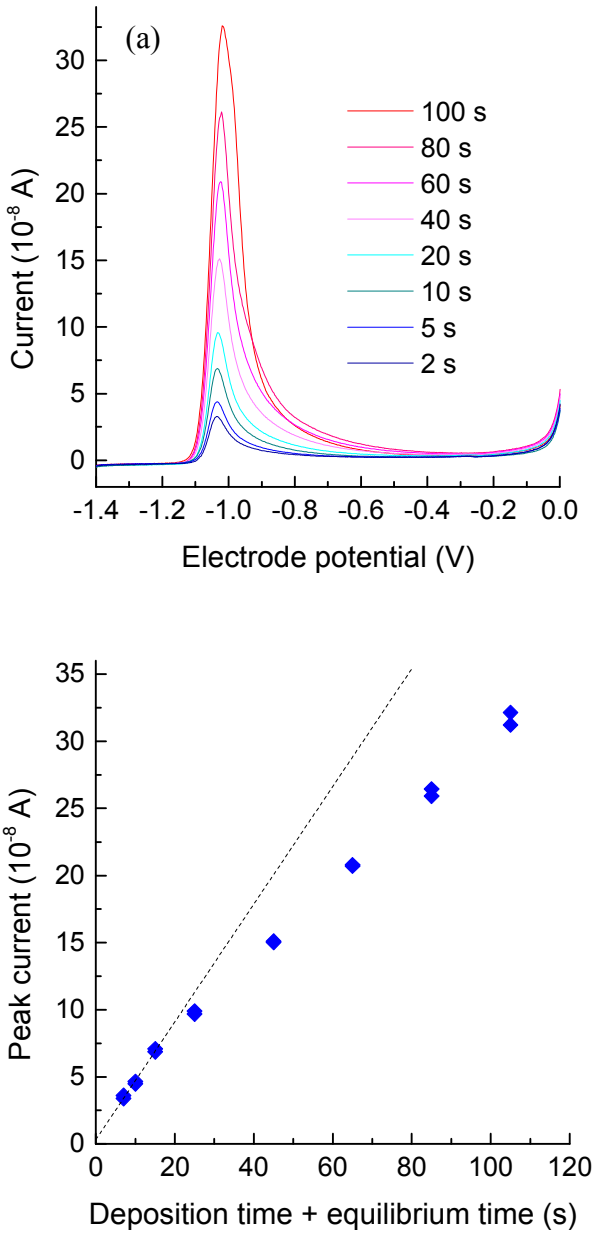

Figure 1. (a) Anodic stripping voltammetric scans and (b) Stripping peak current measured with different deposition times (2-100 s) for a solution containing TES-21 ZnO NP. Scan rate: 0.1 V s^{-1}. Medium: 82 mM KCl solution buffered with 10 mM POPSO. I = 0.1 M, pH = 8.6. T = 25 ºC. Dissolved zinc concentration measured by ASV was 4.1±0.1 µM. Total added ZnO NP was 85 µM. The dashed line in part (b) corresponds to a linear regression of the first three data points.

The effect of potential scan rate on stripping current was also non-linear (**Figure 2**), and peak position shifted slightly from -1.05 V to -1.03 V as the scan rate increased from 0.01 V s^{-1}

to 0.4 V s^{-1}. The increase of peak current with scan rate was fitted to a power law function, with an exponent of 0.46 that is close to the expected theoretical value of 0.5.[38] For scan rates greater than 0.1 V s^{-1}, the stripping current "baseline" was elevated on the positive side of the oxidation peak, suggesting an insufficient time frame (3-6 s) during the potential scan for complete oxidation of the Zn-Hg amalgam.

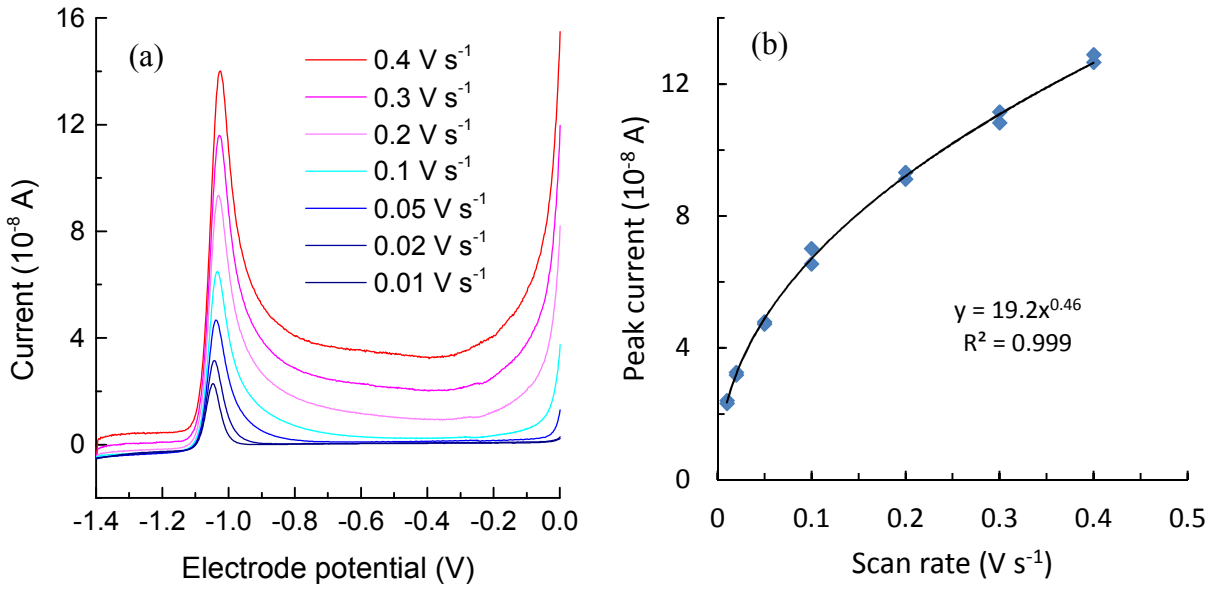

Figure 2. . (a) Anodic stripping voltammetric scans and (b) stripping peak current measured with different potential scan rates (0.01-0.4 V s^{-1}) for a solution containing TES-21 ZnO NP. Deposition time: 10 s. Other experimental conditions, including total and dissolved zinc concentrations, were the same as **Figure 1**.

At the end of these measurements that varied the deposition time and the scan rates (a 3 h experiment in total), the total Zn concentration (22.1 μM) measured in an aliquot of the sample by ICP-MS was much lower than the nominally added value (85 μM). This low recovery of the added Zn indicated that a significant portion of the ZnO NPs settled to the bottom or adsorbed to the glass electrochemical cell. Subsequent dissolution experiments (**Figures 3** to **6**), were carried out in shorter time frames (e.g. < 1.5 h), and higher proportions (approximately 70% to 120%) of

the added ZnO NPs were quantified in aliquots of the sample at the end of the experiments (**Figure S3**).

Comparison between ASV and ultracentrifugation/ICP-MS. Although the above tests were consistent with expectations for the quantification of dissolved species, further comparisons were performed with ultracentrifugation/ICP-MS to determine whether ASV can accurately measure dissolved zinc concentration in the presence of ZnO NPs.

As shown in **Figure 3**, the dissolved Zn concentration measured by ASV ($[Zn]_{ASV}$) was largely consistent with the dissolved Zn quantified by ultracentifugation/ICP-MS ($[Zn]_{ICP\text{-}MS}$). The exceptions were for the smallest nanoparticles. $[Zn]_{ASV}$ was 20% higher than $[Zn]_{ICP\text{-}MS}$ for PVP-4 and Ac-5, with absolute differences of 7-8 μM, suggesting that these small ZnO NPs contributed to measured $[Zn]_{ASV}$. On the other hand, for the larger ZnO NPs, i.e. PVP-21 and TES-21, $[Zn]_{ASV}$ was (79±19)% of $[Zn]_{ICP\text{-}MS}$, with differences of 0-2 μM (on average 1.1±0.7 μM), despite the high concentrations of ZnO NPs in suspension (approximately 50 μM in buffered KCl solution without SRFA, 80 μM with SRFA or 70 μM in filtered wetland water) (**Figure S3** and **Figure S4**). Control experiments showed that total zinc concentration in ASV calibration solutions measured before and after ultracentrifugation was on average (92±9)% and (94±11)% of nominal concentration (**Figure S5** and **Figure S6**), indicating that little dissolved zinc was lost to the electrochemical cell or during ultracentrifugation. Thus, ASV can measure dissolved zinc concentration with sufficient accuracy in the presence of ZnO NPs that are large enough (e.g. larger than 20 nm), in the tested media.

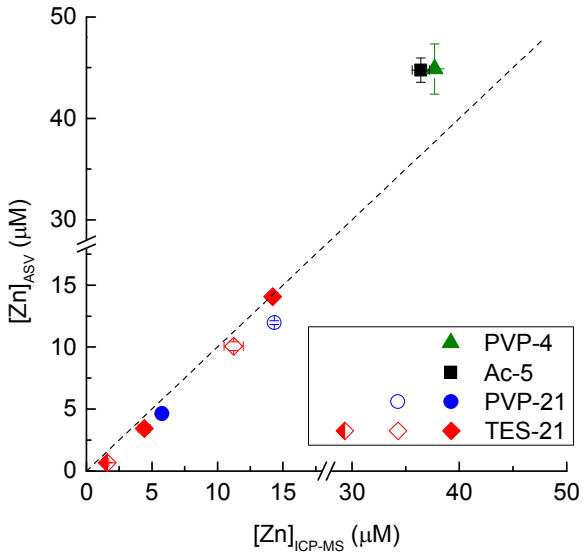

Figure 3. Equilibrium dissolved zinc concentration from different NPs measured by ASV ($[Zn]_{ASV}$) as compared with that measured by ICP-MS after ultracentrifugation ($[Zn]_{ICP-MS}$). Medium: 82 mM KCl solution buffered with 20 mM MOPS or 10 mM POPSO (I = 0.1 M, pH = 8.3-8.6) or filtered wetland water ($I \approx$ 1 mM, pH = 9). T = 25 ºC. Nominal total zinc concentration: 75-290 μM. The dashed line represents the 1:1 line. Closed symbols correspond to experiments conducted without Suwanee River fulvic acid (SRFA), while the open symbols correspond to experiments with 20 mg-C L^{-1} SRFA. The half-filled symbol represents the experiment conducted in filtered wetland suface water.

The need to purge dissolved oxygen from the sample prior to voltammetric analysis could be a limitation of this method to discern dissolved Zn from nanoparticulate zinc. As noted in the Experimental section, the pH of the wetland surface water sample was unstable during the purging step, likely from loss of dissolved CO_2 as the dominant buffer in this matrix. Thus, if ASV were to be applied to distinguish dissolved Zn from colloidal Zn, the composition of the water (e.g., pH) should be tracked to ensure that the resulting data can be interpreted correctly.

Dissolution of four types of ZnO NPs. The 4 types of ZnO NPs had different solubility and dissolution rates at pH 8.6 in the absence of SRFA (**Figure 4**). TES-21 was the slowest to reach equilibrium (approximately 1 h). In contrast, PVP-21 reached equilibrium within 20 min

even though the average d_{TEM} was very close for both of these ZnO NPs. Ac-5 dissolved even faster, and dissolution equilibrium was reached no later than a few minutes.

For PVP-4, dissolved zinc concentration measured by ASV decreased in the first 20 min and then reached a steady state. This initial decrease was probably not due to precipitation and loss of zinc ions from the dissolved phase, since the fraction of dissolved zinc in the stock suspension was very small (<1%) (**Table S1**) and equivalent to less than 0.5 μM of initial dissolved zinc in the dissolution reaction mixture. Instead, this phenomenon was likely caused by the contribution of small NPs to the $[Zn]_{ASV}$ value.

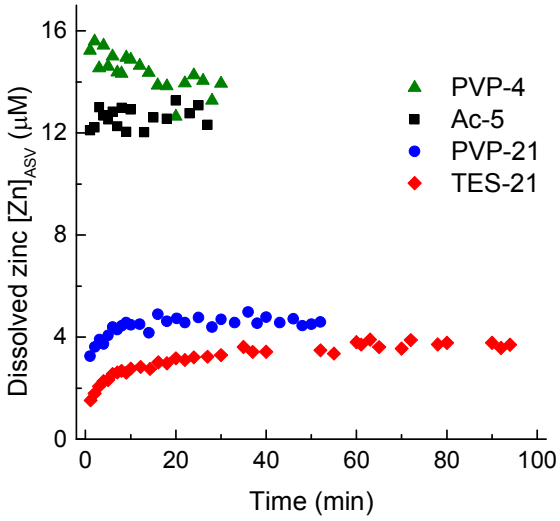

Figure 4. Release of dissolved Zn ($[Zn]_{ASV}$), as quantified by anodic stripping voltammetry with different types of ZnO NPs. Medium: 81-82 mM KCl solution buffered with 20 mM MOPS or 10 mM POPSO. I = 0.1 M, pH = 8.6. T = 25 ºC. Nominal total zinc concentration: 75 μM.

The solubility product (K_{sp}) of the ZnO NPs (for $ZnO_{(s)} + H_2O = Zn^{2+} + 2OH^-$) was calculated from the solution pH and equilibrium total dissolved zinc concentration measured by ASV (as shown in **Figure 3** and **Figure 4**). The calculation followed previously published procedures[18] and are described in detail in the Supporting Information. Dissolution data for PVP-

4 and Ac-5 ZnO NPs resulted in K_{sp} values close to 4.5×10^{-17} (**Table S4**), which is consistent with previously reported K_{sp} values of ZnO NPs of similar size.[18, 47] The PVP-21 and TES-21 ZnO NPs also had similar K_{sp} values (1.4×10^{-17} and 1.0 to 1.5×10^{-17}, respectively), which are much lower than that for the smaller ZnO NPs, yet also generally consistent with reported values of ZnO NPs of similar size.[18, 47] These data confirm that the solubility product of the ZnO NPs is strongly dependent on their primary particle size,[18, 47] and indicate that surface coatings has little effect on the solubility product, especially if the coatings do not form an impermeable layer on the surface of the NPs.[48]

While the solubility product values from this study were largely consistent with previous work, the approximate rates of dissolution were not fully consistent with the literature. In previous studies with ZnO NPs, the time needed to reach dissolution equilibrium ranged from less than 1 h[18, 49, 50] to several hours.[12, 47, 51, 52] In some cases, dissolution was very slow, and equilibrium was not reached after days,[48] and even more than a month.[53] Dissolution rates of ZnO NPs can depend on mixing conditions, the concentration of NP surface area available for dissolution (as influenced by the mass/molar concentration,[11, 52] primary particle size,[18] surface coating,[50, 54] and aggregation state of the ZnO NPs), and water chemistry of the media,[10, 12, 48, 51, 53-56] especially pH and Zn-chelating ligands. The wide range of dissolution rates in these studies may be due to these differences. However, we note that the separation methods used in most of the studies utilized centrifugation and/or filtration, neither of which allows for short time resolutions needed for ZnO NP dissolution kinetics study. As such, electrochemical methods described here and in a previous study[18] are more suitable for discerning the kinetics of nanoparticle dissolution and the influence of processes such as nanoparticle aggregation state and water composition.

Influence of aggregation state on ZnO NP dissolution. Aggregation of nanoparticles could influence the interactions of the nanoparticles with the hanging mercury drop electrode and also the available surface area for dissolution. For samples with the PVP-4 ZnO NPs, the particles appeared to aggregate upon addition into the KCl solution (**Figure S7**). In the initial stage, the polydispersity index (PDI) was very high (> 0.6), indicating a very broad size distribution of the ZnO NP aggregates, which included small aggregates. Then over the course of 30 min, the Z-average hydrodynamic diameter increased from 800 nm to 1000 nm and the PDI decreased from 0.6 to 0.3. These results indicated that the particles continued to aggregate and the very large aggregates were likely settling from solution. Thus, the decrease in the number of small particles during aggregation could explain the decrease in $[Zn]_{ASV}$ over time for PVP-4 ZnO NP (**Figure 4**).

The initial aggregation state of the nanoparticle stock suspension appeared to influence the dissolution kinetics during the experiments. For experiments performed with individually dispersed NP stock suspensions (**Figure 4**), the small ZnO NPs dissolved extremely quickly, even though aggregation occurred immediately after ZnO NP stock suspension was added to the KCl buffer solution. This aggregation is likely to be diffusion-limited, resulting in loose ZnO NP aggregates with low fractal dimension.[57] Furthermore, the stirring and N_2 purging in the experiment probably resulted in surface-controlled dissolution of ZnO NPs rather than transport-controlled dissolution.[58] In contrast, for Ac-5 ZnO NP stock suspensions that had undergone irreversible aggregation (with d_h of 98 nm in the stock suspension), dissolution was much slower under the same conditions, and equilibrium was not reached until after 15-20 min (**Figure 5**), suggesting that dissolution kinetics was limited by the diffusion of ions away from aggregated ZnO NPs and into bulk solution.

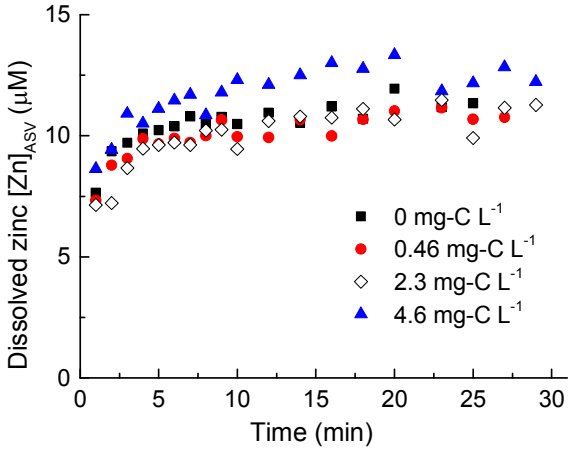

Figure 5. Dissolution of Ac-5 ZnO NPs with different concentrations of SRFA. Medium: 81 mM KCl solution buffered with 20 mM MOPS. I = 0.1 M, pH = 8.6. T = 25 ºC. Nominal total zinc concentration: 75 μM.

Influence of fulvic acid on ZnO NP dissolution. The presence of 4.6 mg-C L^{-1} SRFA in the dissolution reaction mixture significantly reduced aggregation of the nanoparticles (**Figure S8**), but the effect on ZnO NP dissolution was not drastic (**Figure 5**). When Ac-5 ZnO NPs were mixed in the buffer solution with SRFA (4.6 mg-C L^{-1}), the dissolved Zn concentration was approximately 12.5±0.6 μM at 20-25 min, slightly higher than the control with no SRFA ($[Zn]_{ASV}$ = 11.5±0.4 μM at 20-30 min). Likewise at pH 7.9 and 8.3, ZnO NP solubility increased relative to the experiment at pH 8.6, but SRFA still had no significant effect on ZnO NP dissolution at concentrations up to 4.6 mg-C L^{-1} (**Figure S9**).

The effect of NOM on mineral dissolution depends on the amount of NOM relative to the mineral surface area,[59] and not just mass concentration ratio. Thus, we further tested the effect of SRFA on the dissolution of TES-21 ZnO NPs, which had lower specific area and solubility. As SRFA concentration increased from 0 to 40 mg-C L^{-1}, both peak height and peak area of the stripping current in the calibration solutions decreased (**Figure S10**).This result indicates that the presence of SRFA suppressed the ASV signal for Zn, likely due to the formation of Zn-SRFA

416 complexes that are less reactive during the voltammmetric measurement. The decreased peak
417 current signal was taken into account by using separate Zn calibration curves for each
418 corresponding matrix (i.e. **Figure S10**). With this correction, the dissolution experiments with
419 TES-21 ZnO NPs showed that Zn solubility (as indicated by the equilibrium $[Zn]_{ASV}$) increased
420 with SRFA concentration (**Figure 6**).

421 In a previous study,[10] SRFA was reported to inhibit the dissolution of ZnO NP (primary
422 particle size: 20 nm; total concentration: 6.14 mM) in artificial sea water at 2.6 mg-C L^{-1}, but
423 promoted ZnO NP dissolution at 26 mg-C L^{-1}. The effect of SRFA at both concentrations on
424 ZnO NP solubility (measured after 2 d in this previous study) was not obvious, considering the
425 variance of the measurements,[10] and this may partly be due to the low SRFA to ZnO NP ratio
426 used in that study. The concentrations of ZnO NPs in most aquatic environments are low (e.g. on
427 the order of 10^{-2} ug L^{-1} in surface water and 1 ug L^{-1} in waste water treatment plant effluents),[60]
428 although they are expected to increase with the wider application and disposal of consumer and
429 industrial products containing ZnO NPs.[61] On the other hand, the concentration of dissolved
430 organic matter in natural and engineered aquatic systems can span from 1 to 60 mg-C L^{-1}.[40]
431 Therefore, high NOM to ZnO NP ratios are expected, and as a result, can have significant
432 influence on the dissolution and transformation of ZnO NPs.

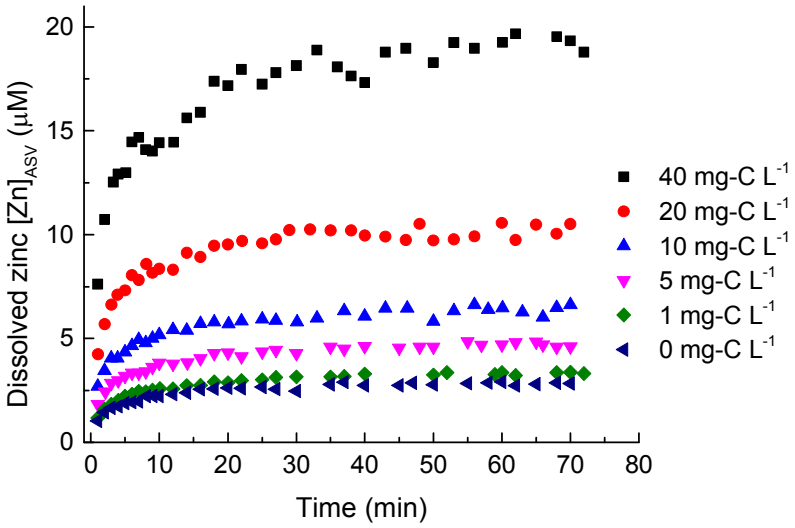

Figure 6. Dissolution of TES-21 ZnO NPs with different concentrations of SRFA. Medium: 82 or 91 mM KCl solution buffered with 10 or 5 mM POPSO. I = 0.1 M, pH = 8.6. T = 25 ºC. Nominal total zinc concentration: 75 µM.

Conclusions

This study demonstrated the competence of ASV to directly measure dissolved zinc concentration in ZnO NP suspensions without the need for separation of the particulate phase from the aqueous phase. This separation process has been a critical yet challenging step in most other methods to measure dissolved zinc concentration in nanoparticle suspensions. This *in situ* measurement with ASV allows for higher time resolution (i.e. on the order of 1 min) than the methods involving the separation of nanoparticles, making ASV a more suitable method to study the dissolution kinetics of ZnO NPs, especially in complex matrices such as natural waters containing dissolved organic matter or culture media used for toxicity assays. The application of ASV, however, requires that the calibration solutions have the same matrix as the samples.

In addition to zinc, ASV may also be used to measure dissolved concentration of other metals of environmental concern, such as copper, lead and cadmium,[23] in the presence of engineered nanoparticles or naturally occurring mineral colloids containing these metals. The

application of ASV in the dissolution study of metal-based nanoparticles may provide useful information regarding their environmental fate, bioavailability and toxicity.

Acknowledgements

The work was supported by the National Science Foundation (NSF) (CBET-1066781). Additional support was provided by the Center for the Environmental Implications of NanoTechnology (CEINT), funded by the NSF and the U.S. EPA (EF-0830093). Any opinions, findings, conclusions, or recommendations expressed in this material are those of the author(s) and do not necessarily reflect the views of the NSF or the EPA. This work has not been subjected to EPA review and no official endorsement should be inferred.

References

1. M. R. Wiesner, G. V. Lowry, P. Alvarez, D. Dionysiou and P. Biswas, *Environmental Science & Technology*, 2006, 40, 4336-4345.
2. C. Hariharan, *Applied Catalysis A-General*, 2006, 304, 55-61.
3. M. J. Osmond and M. J. McCall, *Nanotoxicology*, 2010, 4, 15-41.
4. R. Brayner, R. Ferrari-Iliou, N. Brivois, S. Djediat, M. F. Benedetti and F. Fievet, *Nano Letters*, 2006, 6, 866-870.
5. H. B. Ma, P. L. Williams and S. A. Diamond, *Environmental Pollution*, 2013, 172, 76-85.
6. N. M. Franklin, N. J. Rogers, S. C. Apte, G. E. Batley, G. E. Gadd and P. S. Casey, *Environmental Science & Technology*, 2007, 41, 8484-8490.
7. S. W. Y. Wong, P. T. Y. Leung, A. B. Djurisic and K. M. Y. Leung, *Analytical and Bioanalytical Chemistry*, 2010, 396, 609-618.
8. W. H. Song, J. Y. Zhang, J. Guo, J. H. Zhang, F. Ding, L. Y. Li and Z. T. Sun, *Toxicology Letters*, 2010, 199, 389-397.
9. B. Wu, Y. Wang, Y. H. Lee, A. Horst, Z. P. Wang, D. R. Chen, R. Sureshkumar and Y. J. J. Tang, *Environmental Science & Technology*, 2010, 44, 1484-1489.
10. A. J. Miao, X. Y. Zhang, Z. P. Luo, C. S. Chen, W. C. Chin, P. H. Santschi and A. Quigg, *Environmental Toxicology and Chemistry*, 2010, 29, 2814-2822.
11. R. J. Miller, H. S. Lenihan, E. B. Muller, N. Tseng, S. K. Hanna and A. A. Keller, *Environmental Science & Technology*, 2010, 44, 7329-7334.
12. M. Li, L. Z. Zhu and D. H. Lin, *Environmental Science & Technology*, 2011, 45, 1977-1983.
13. P. Wang, N. W. Menzies, E. Lombi, B. A. McKenna, B. Johannessen, C. J. Glover, P. Kappen and P. M. Kopittke, *Environmental Science & Technology*, 2013, 47, 13822-13830.
14. X. S. Zhu, J. X. Wang, X. Z. Zhang, Y. Chang and Y. S. Chen, *Nanotechnology*, 2009, 20.
15. C. W. Lee, S. Mahendra, K. Zodrow, D. Li, Y. C. Tsai, J. Braam and P. J. J. Alvarez, *Environmental Toxicology and Chemistry*, 2010, 29, 669-675.
16. P. Y. Chen, B. A. Powell, M. Mortimer and P. C. Ke, *Environmental Science & Technology*, 2012, 46, 12178-12185.
17. H. C. Poynton, J. M. Lazorchak, C. A. Impellitteri, B. Blalock, M. E. Smith, K. Struewing, J. Unrine and D. Roose, *Environmental Science & Technology*, 2013, 47, 9453-9460.
18. C. A. David, J. Galceran, C. Rey-Castro, J. Puy, E. Companys, J. Salvador, J. Monne, R. Wallace and A. Vakourov, *Journal of Physical Chemistry C*, 2012, 116, 11758-11767.
19. M. S. Xu, J. Li, N. Hanagata, H. X. Su, H. Z. Chen and D. Fujita, *Nanoscale*, 2013, 5, 4763-4769.
20. G. R. Aiken, H. Hsu-Kim and J. N. Ryan, *Environmental Science & Technology*, 2011, 45, 3196-3201.
21. A. Zirino and M. L. Healy, *Limnology and Oceanography*, 1971, 16, 773-&.
22. G. Gillain, G. Duyckaerts and A. Disteche, *Anal. Chim. Acta*, 1979, 106, 23-37.
23. C. M. G. van den Berg, *Anal. Chim. Acta*, 1991, 250, 265-276.
24. P. J. S. Barbeira, L. H. Mazo and N. R. Stradiotto, *Analyst*, 1995, 120, 1647-1650.
25. I. Ciglenecki, E. Bura-Nakic and M. Margus, *J. Solid State Electrochem.*, 2012, 16, 2041-2046.

26. C. M. G. van den Berg, A. G. A. Merks and E. K. Duursma, *Estuar. Coast. Shelf Sci.*, 1987, 24, 785-797.
27. C. M. G. van den Berg, M. Boussemart, K. Yokoi, T. Prartono and M. Campos, *Mar. Chem.*, 1994, 45, 267-282.
28. E. Deaver and J. H. Rodgers, *Environmental Toxicology and Chemistry*, 1996, 15, 1925-1930.
29. A. Bobrowski, B. Bas, J. Dominik, E. Niewiara, E. Szalinska, D. Vignati and J. Zarebski, *Talanta*, 2004, 63, 1003-1012.
30. H. B. Jung, S. T. Yun, S. O. Kim, M. C. Jung, C. S. So and Y. K. Koh, *Environ. Geochem. Health*, 2006, 28, 283-296.
31. P. J. Brendel and G. W. Luther, *Environmental Science & Technology*, 1995, 29, 751-761.
32. I. Ciglenecki, D. Krznaric and G. R. Helz, *Environmental Science & Technology*, 2005, 39, 7492-7498.
33. E. Bura-Nakic, D. Krznaric, D. Jurasin, G. R. Helz and I. Ciglenecki, *Anal. Chim. Acta*, 2007, 594, 44-51.
34. B. P. Colman, B. Espinasse, C. J. Richardson, C. W. Matson, G. V. Lowry, D. E. Hunt, M. R. Wiesner and E. S. Bernhardt, *Environmental Science & Technology*, 2014, 48, 5229-5236.
35. E. A. Meulenkamp, *Journal of Physical Chemistry B*, 1998, 102, 5566-5572.
36. L. Guo, S. H. Yang, C. L. Yang, P. Yu, J. N. Wang, W. K. Ge and G. K. L. Wong, *Applied Physics Letters*, 2000, 76, 2901-2903.
37. C. M. Wu, J. Baltrusaitis, E. G. Gillan and V. H. Grassian, *Journal of Physical Chemistry C*, 2011, 115, 10164-10172.
38. J. Wang, *Analytical Electrochemistry*, Wiley-VCH, 3 edn., 2006.
39. E. P. Achterberg and C. Braungardt, *Anal. Chim. Acta*, 1999, 400, 381-397.
40. A. A. Keller, H. T. Wang, D. X. Zhou, H. S. Lenihan, G. Cherr, B. J. Cardinale, R. Miller and Z. X. Ji, *Environmental Science & Technology*, 2010, 44, 1962-1967.
41. C. M. G. van den Berg, *Talanta*, 1984, 31, 1069-1073.
42. C. M. G. van den Berg and Q. H. Zi, *Anal. Chem.*, 1984, 56, 2383-2386.
43. C. M. G. van den Berg and Z. Q. Huang, *J. Electroanal. Chem.*, 1984, 177, 269-280.
44. C. M. G. van den Berg, *Anal. Chim. Acta*, 1984, 164, 195-207.
45. K. Yokoi and C. M. G. Van Den Berg, *Anal. Chim. Acta*, 1991, 245, 167-176.
46. M. Campos and C. M. G. Van Den Berg, *Anal. Chim. Acta*, 1994, 284, 481-496.
47. I. A. Mudunkotuwa, T. Rupasinghe, C. M. Wu and V. H. Grassian, *Langmuir*, 2012, 28, 396-403.
48. R. Ma, C. Levard, F. M. Michel, G. E. Brown and G. V. Lowry, *Environmental Science & Technology*, 2013, 47, 2527-2534.
49. X. O. Zheng, R. Wu and Y. G. Chen, *Environmental Science & Technology*, 2011, 45, 2826-2832.
50. T. Buerki-Thurnherr, L. S. Xiao, L. Diener, O. Arslan, C. Hirsch, X. Maeder-Althaus, K. Grieder, B. Wampfler, S. Mathur, P. Wick and H. F. Krug, *Nanotoxicology*, 2013, 7, 402-416.
51. J. T. Lv, S. Z. Zhang, L. Luo, W. Han, J. Zhang, K. Yang and P. Christie, *Environmental Science & Technology*, 2012, 46, 7215-7221.
52. W. M. Li and W. X. Wang, *Water Research*, 2013, 47, 895-902.

53. R. B. Reed, D. A. Ladner, C. P. Higgins, P. Westerhoff and J. F. Ranville, *Environmental Toxicology and Chemistry*, 2012, 31, 93-99.
54. A. Gelabert, Y. Sivry, R. Ferrari, A. Akrout, L. Cordier, S. Nowak, N. Menguy and M. F. Benedetti, *Environmental Toxicology and Chemistry*, 2014, 33, 341-349.
55. T. Xia, M. Kovochich, M. Liong, L. Madler, B. Gilbert, H. B. Shi, J. I. Yeh, J. I. Zink and A. E. Nel, *ACS Nano*, 2008, 2, 2121-2134.
56. S. W. Bian, I. A. Mudunkotuwa, T. Rupasinghe and V. H. Grassian, *Langmuir*, 2011, 27, 6059-6068.
57. D. X. Zhou and A. A. Keller, *Water Research*, 2010, 44, 2948-2956.
58. G. Sposito, *The Surface Chemistry of Natural Particles*, Oxford University Press, 2004.
59. J. S. Waples, K. L. Nagy, G. R. Aiken and J. N. Ryan, *Geochimica Et Cosmochimica Acta*, 2005, 69, 1575-1588.
60. F. Gottschalk, T. Y. Sun and B. Nowack, *Environmental Pollution*, 2013, 181, 287-300.
61. A. A. Keller, S. McFerran, A. Lazareva and S. Suh, *Journal of Nanoparticle Research*, 2013, 15.